Available online at www.sciencedirect.com
ScienceDirect
Journal of Power Sources 171 (2007) 793–801
JOURNAL OF POWER SOURCES
www.elsevier.com/locate/jpowsour

Development and experimental characterization of a fuel cell powered aircraft

Thomas H. Bradley *, Blake A. Moffitt, Dimitri N. Mavris, David E. Parekh

Georgia Institute of Technology, Atlanta, GA 30332-0405, United States

Received 24 April 2007; received in revised form 23 May 2007; accepted 4 June 2007
Available online 1 July 2007

Abstract

This paper describes the characteristics and performance of a fuel cell powered unmanned aircraft. The aircraft is novel as it is the largest compressed hydrogen fuel cell powered airplane built to date and is currently the only fuel cell aircraft whose design and test results are in the public domain. The aircraft features a 500 W polymer electrolyte membrane fuel cell with full balance of plant and compressed hydrogen storage incorporated into a custom airframe. Details regarding the design requirements, implementation and control of the aircraft are presented for each major aircraft system. The performances of the aircraft and powerplant are analyzed using data from flights and laboratory tests. The efficiency and component power consumption of the fuel cell propulsion system are measured at a variety of flight conditions. The performance of the aircraft powerplant is compared to other 0.5–1 kW-scale fuel cell powerplants in the literature and means of performance improvement for this aircraft are proposed. This work represents one of the first studies of fuel cell powered aircraft to result in a demonstration aircraft. As such, the results of this study are of practical interest to fuel cell powerplant and aircraft designers.

Keywords: Fuel cell; Aviation; Vehicle; Experiment; Unmanned aerial vehicle

1. Introduction

Long-endurance unmanned aerial vehicles (UAVs) are a subject of interest among the aerospace community because of their potential to accomplish a variety of telecommunications, reconnaissance and remote sensing missions. Compared to space-based satellites, long-endurance UAVs can exhibit lower capitol costs, faster mission cycle time and greater mission adaptability [1]. At present, a majority of long-endurance aircraft are powered by conventional gas turbine powerplants [2].

Polymer electrolyte membrane (PEM) fuel cell powerplants powered by compressed or liquefied hydrogen have particular advantages over other technologies available for long-endurance aircraft because fuel cell systems can exhibit high specific energy, high efficiency and can be incorporated into rechargeable energy storage systems. For example, a conventional gasoline-fueled internal combustion powerplant at the scale of the aircraft considered for this project (fuel consumption 0.5 g s^{-1} at 375 W cruise, 0.489 kg engine [3], 10 h endurance) has a specific mechanical energy of approximately 200 Wh kg^{-1}. PEM fuel cells with compressed gaseous hydrogen or liquid hydrogen storage can exhibit specific electrical energies of 1000 Wh kg^{-1} [4] and >10,000 Wh kg^{-1}, respectively [5]. For rechargeable systems, advanced batteries can reach electrical output specific energies of 200 Wh kg^{-1} at the module level [6] and have charge–discharge efficiencies of nearly 100% at low current [7]. A fuel cell/electrolyzer rechargeable fuel cell system with compressed hydrogen storage can have a specific electrical energy of >800 Wh kg^{-1} [8,9], a charge efficiency of 80% and a discharge efficiency of 50% [10]. This results in a round trip, specific electrical energy of >320 Wh kg^{-1}. So, in comparison to conventional technologies, compressed hydrogen fuel cells can exhibit significantly higher specific energy than advanced batteries and small-scale internal combustion engines. Fuel cells with liquid hydrogen storage have significantly greater specific energy than hydrocarbon fueled internal combustion engines.

* Corresponding author at: George W. Woodruff School of Mechanical Engineering, Georgia Institute of Technology, 801 Ferst Drive, Atlanta, GA 30332-0405, United States. Tel.: +1 404 385 9364; fax: +1 404 894 8336.
E-mail address: bradley@gatech.edu (T.H. Bradley).

0378-7753/$ – see front matter © 2007 Elsevier B.V. All rights reserved.
doi:10.1016/j.jpowsour.2007.06.215

Fig. 1. Demonstrator fuel cell aircraft in-flight.

Despite these theoretical advantages of fuel cell aviation powerplants, there exists very little practical knowledge about the implementation challenges associated with making an integrated fuel cell/aircraft system. A primary challenge of fuel cell aircraft design is that specific power (or power-to-weight ratio) is commonly used as a high-level indicator of aircraft performance [11], whereas fuel cell powerplants are generally characterized by low specific power ($W\,kg^{-1}$). This mismatch between the characteristics of the powerplant and the requirements of the vehicle provides strict limits on the power consumption and weight of the powerplant systems, so as to maximize aircraft specific power, and thereby maximize aircraft performance. Fuel cell powered aircraft concepts are therefore characterized by high efficiency airframes, low weight structures, high efficiency propulsion systems, low power payloads and low-margin, highly constrained designs [12–15]. A majority of existing studies of fuel cell powered aircraft are high-level, conceptual design studies where the low-level compromises between the requirements of the aircraft and the characteristics of the powerplant are not made explicitly. A few researchers have proven the viability of small-scale fuel cell powered UAVs by placing fuel cells into model-scale aircraft [16–18]. AeroVironment has designed and demonstrated a large-scale fuel cell UAV in a custom airframe, but details regarding the aircraft and powerplant are not publicly available [19].

Based on the limitations of this previous work, there exists a need for a comprehensive, documented development and performance analysis for a larger-scale fuel cell aircraft. To work towards this goal, the George Woodruff School of Mechanical Engineering, the Georgia Tech Research Institute and the Aerospace Systems Design Laboratory at the Georgia Institute of Technology Daniel Guggenheim School of Aerospace Engineering have designed and built the technology demonstrator fuel cell aircraft shown in Fig. 1. The aircraft itself is novel as it is the largest fuel cell aircraft yet developed that is fueled by compressed hydrogen and the largest fuel cell aircraft whose design and test results are in the public domain.

This aircraft can serve as a platform for development and testing of fuel cell powerplants for aircraft and as a tool for validation of system design models and methodologies. The demonstrator aircraft is designed to comply with the specifications of the Academy of Model Aeronautics. This sets a maximum mass constraint for the aircraft at 24.9 kg and functionally limits the aircraft to testing at model aircraft runways. This scale simplifies the licensing of the aircraft and is appropriate for an academic demonstration project.

The aircraft design was broken down into high-level conceptual and low-level detailed design tasks. The aircraft conceptual design was performed by assembling a series of contributing analyses into a higher level simulation of the fuel cell aircraft performance. The performance simulation is parameterized within a defined, discritized design space to allow variation in the aircraft configurations and subsystem specifications. Because of the high computational load associated with characterizing the design space, simplifying assumptions are built into the contributing analyses. Validation of the conceptual design is critical for ensuring its effectiveness. A more detailed breakdown of the conceptual and low-level design tasks is provided in references [20,21]. The aircraft was constructed based on the results of the detail design.

This paper presents the low-level specifications and performance characteristics of the demonstration aircraft and its power and propulsion systems, as constructed. The fuel cell powerplant system design and aircraft design are presented with performance data that show the interaction between the fuel cell powerplant and vehicle. Flight and laboratory testing results are presented and means of performance improvements are discussed.

2. Powerplant system description

For the demonstrator aircraft, the fuel cell is the only source of propulsive power. The fuel cell powerplant designed for use in the demonstrator aircraft is composed of the fuel cell stack, thermal management, air management, and hydrogen storage and management subsystems, as shown in Fig. 2. These subsystems are controlled by an ATMEGA32, 8-bit AVR microcontroller module (Atmega, San Jose, CA) that functions as both the powerplant controller and the aircraft data acquisition system.

A summary of the powerplant characteristics as constructed is presented in Table 1. The balance of plant configuration shown in Fig. 2, which includes a dead-ended anode, liquid cooling,

Table 1
Fuel cell system characteristics

Powerplant specification	Value
PEM fuel cell stack	
Number of cells	32
Cell active area (cm^2)	64
Operating temperature (°C)	60
Mass (kg)	4.96
Hydrogen storage	
Storage pressure (MPa)	31
Capacity (SL)	192
Powerplant system	
Peak output power (W)	465
Specific electrical energy ($Wh\,kg^{-1}$)	7.1
Specific electrical power ($W\,kg^{-1}$)	52

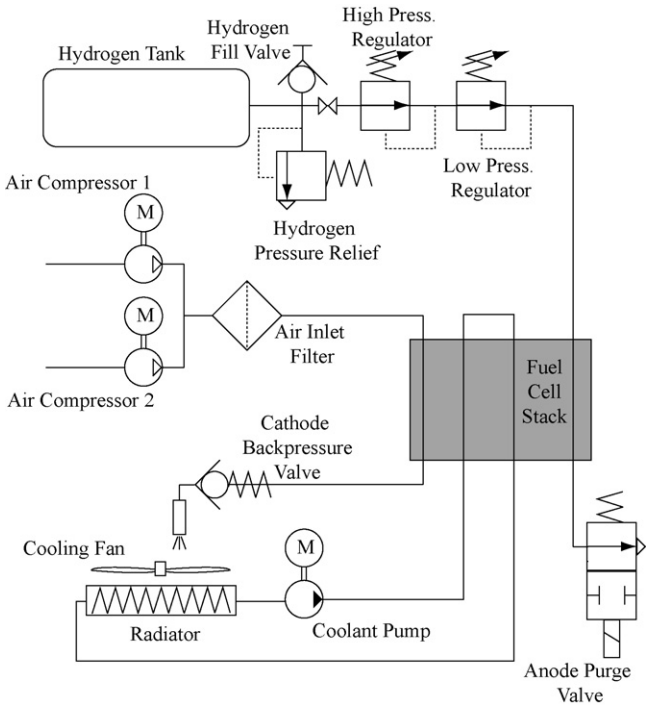

Fig. 2. Fuel cell powerplant diagram and system specifications.

pressurized cathode and active air flow control, was chosen so that the powerplant incorporates the same subsystems that are required to control PEM fuel cell systems of much higher power. Although there are fuel cell systems with comparable power output that are passively controlled or incorporate simplified balance of plant systems, using a more complete balance of plant improves the applicability and generalization of the design tools developed and lessons learned for this project.

The following sections describe the components, design and specifications of the fuel cell powerplant subsystems.

2.1. Fuel cell stack

The fuel cell stack converts the chemical energy of stored hydrogen and ambient oxygen to electricity. The fuel cell powerplant for the demonstrator fuel cell aircraft is derived from the 500 W 32-cell PEM self-humidified hydrogen-air fuel cell manufactured by BCS Technology Inc. (Bryan, TX). A photograph of the fuel cell stack is shown in Fig. 3. The fuel cell uses membranes from De Nora Inc. (Somerset, NJ) and a proprietary membrane electrode assembly production process designed to improve the water carrying capacity of the membrane [22]. The active area of each membrane electrode assembly is 64 cm^2. The graphite bipolar plates incorporate a triple-serpentine flow channel design, and liquid cooling channels. The fuel cell endplates are of a custom design to reduce the weight of the fuel cell and to simplify its mounting in the aircraft. The fuel cell stack performance without balance of plant loads is shown in Fig. 4. The modifications to the stack that were required to incorporate the stack into the aircraft have no measurable effect on the electronic resistance or electrochemical performance of the stack.

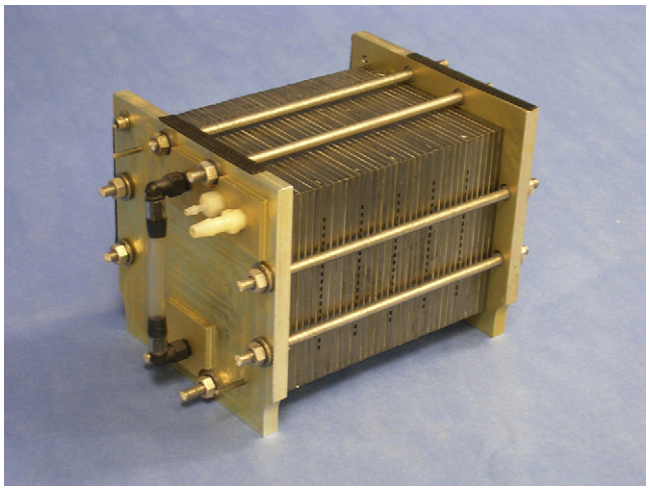

Fig. 3. Customized 32-cell fuel cell stack.

2.2. Temperature control system

The purpose of the temperature control system is to maintain the temperature of the fuel cell stack within a range dictated by the fuel cell performance. When the fuel cell temperature is too low, the activation and mass transport overpotential is high. When the fuel cell temperature is too high (greater than approximately 65 °C), the self-humidification function of the fuel cell begins to break down. The lack of liquid water decreases the protonic conductivity of the fuel cell membrane, degrading performance [23].

A liquid cooling circuit circulates deionized water through the fuel cell, water pump and radiator. There is no contact between the deionized water of the cooling circuit and the fuel cell reactants or product water. The water pump (Laing DDC, Chula Vista, CA) circulates 1.5 L min^{-1} of water at the pressure drop of the fuel cell, radiator and couplings.

The fuel cell radiator is constructed of internally finned aluminum tubing with carbon foam (Poco Graphite, 0.56 g cm^{-3})

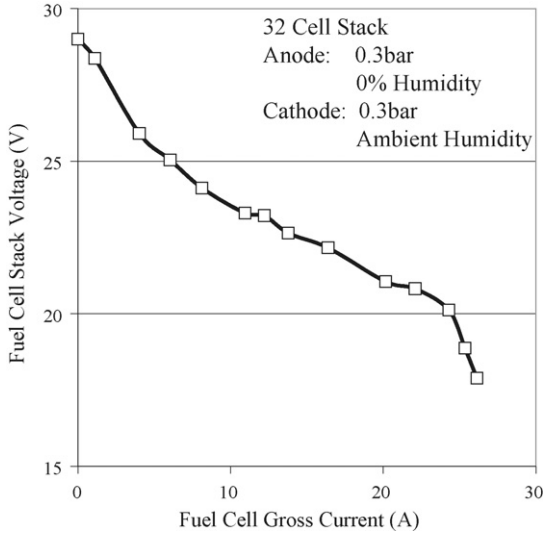

Fig. 4. Fuel cell stack polarization curve.

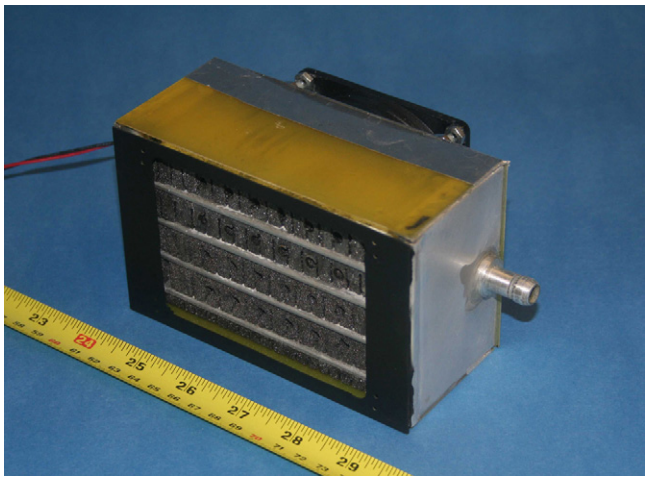

Fig. 5. Carbon foam radiator.

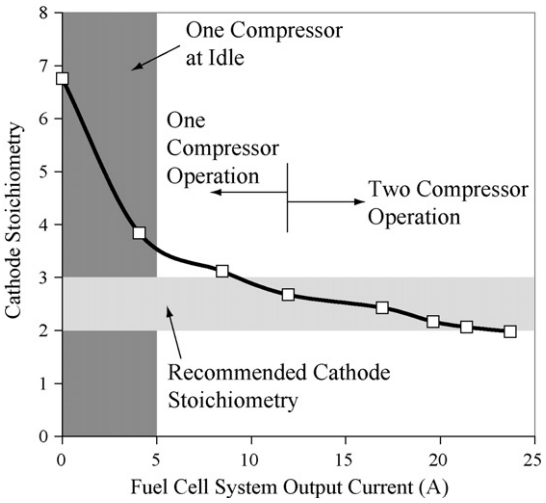

Fig. 6. Cathode stoichiometry as a function of fuel cell system output current.

providing the air to aluminum interface. A photograph of the radiator is shown in Fig. 5. The carbon foam is cut into banks of fins and is pressed to the aluminum tubes. Air from the outside of the aircraft fuselage is ducted through the radiator by an 80 mm diameter, 3 W fan. The carbon foam is continuously wetted with the fuel cell product water to enable evaporative cooling of the radiator. Development of the custom carbon foam radiator resulted in a weight savings of 500 g and a power savings of 12 W when compared to conventional aluminum radiators.

2.3. Air management system

The air management system provides filtered and pressurized air to the cathode manifolds of the fuel cell with variable flow rate control. Variable flow rate control is particularly important in a self-humidified fuel cell system because of the risk of under-humidification at low current densities. For the self-humidified fuel cell, there are no humidification requirements for the reactant gases and the air enters the fuel cell at the ambient humidity ratio.

The 0.3 bar cathode pressure is regulated with a calibrated, spring loaded, ball check valve (Microchek 14B14B-5psi, Lodi, CA). Flow rate is controlled by pulse-width modulation of two diaphragm compressors (T-Squared Manufacturing T202, Lincoln Park, NJ). These compressors are powered from the fuel cell bus voltage. By using two compressors, and turning one of the compressors off when low flow is required, higher high flow rates and lower low flow rates are achievable than is possible with a single compressor. Fig. 6 shows the cathode stoichiometric ratio provided by the compressors as a function of the fuel cell output current. A cathode stoichiometry between 2.0 and 3.0 is recommended by the fuel cell manufacturer. For fuel cell system currents over 12 A, both compressors are used. Under 12 A, only one compressor is used. For fuel cell system currents under 5 A, the flow rate is constrained by the idle speed of the compressor, and the recommended stoichiometry cannot be achieved.

2.4. Hydrogen storage/management system

The hydrogen storage and management system stores gaseous hydrogen and delivers the hydrogen to the fuel cell at a controlled pressure and flow rate. Hydrogen is stored on board of the aircraft in a carbon fiber/epoxy cylinder with aluminum tank liner (Luxfer Gas Cylinders P07A, Riverside, CA). The hydrogen tank has an internal volume of 0.74 L. Two inline single-stage regulators (Pursuit Marketing Inc., 40610, Des Plaines, IL and Airtrol Components Inc., ORS810, New Berlin, WI) regulate the hydrogen storage pressure of 310 bar down to the anode manifold delivery pressure of 0.3 bar. A solenoid purge valve (Asco Valve Inc., 407C1424050N, Florham Park, NJ) opens periodically to purge water and contaminants from the anode flow channels. The purge cycle period is an experimentally derived function of the fuel cell output current and is designed to maximize the voltage stability and hydrogen utilization of the stack. The purge cycle pulse width is 0.2 s. Fig. 7 shows the experimentally measured dynamic behavior of the hydrogen flow rate and anode pressure during purge. Pressure and flow rate are measured using an inline flow meter (Omega Engineering Inc., FMA-1610A, Stamford, CT). The pressure

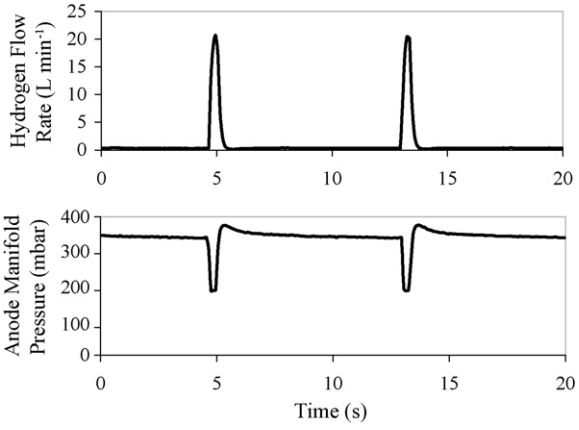

Fig. 7. Dynamic behavior of hydrogen purge under idle conditions.

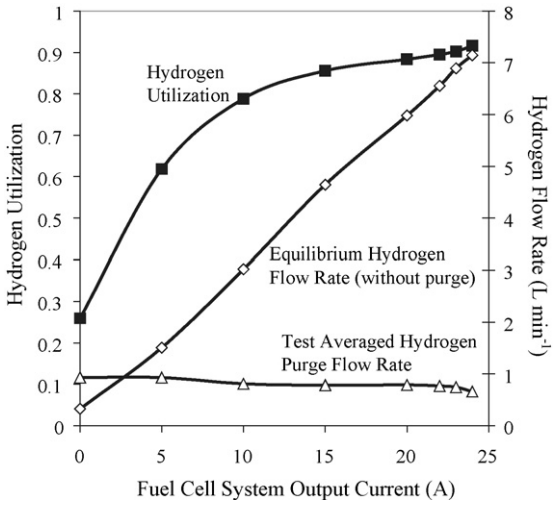

Fig. 8. Hydrogen purge system behavior.

droop during valve opening and the overshoot after valve closing are due to the regulator dynamics. Fig. 8 shows the hydrogen utilization as a function of the fuel cell system output current. The hydrogen utilization is defined by the ratio of the purge hydrogen flow to the total hydrogen flow. Because the hydrogen purge cycle period is only a weak function of the current output of the fuel cell, the anode stoichiometry varies as a function of output current. The peak hydrogen utilization of the stack is 90% and occurs at peak current.

3. Aircraft description

The demonstrator aircraft is designed as a proof-of-concept without a defined payload or endurance requirement. The primary missions of the aircraft are to reliably demonstrate fuel cell powered flight, and gather high-quality repeatable data regarding the function of the aircraft and fuel cell systems. As such, the main requirements of the aircraft are robust flight performance, high stability and fast landing to takeoff turn around time. Even these broad performance requirements place limitations on the conceptual design of the aircraft. For instance, landing gear are used for the demonstrator aircraft despite their added weight and drag because they allow the aircraft to be reliably landed and redeployed without repair or reconfiguration.

The following sections describe the design requirements, and specifications of important aspects of an aircraft designed for use with a fuel cell powerplant.

3.1. Aerodynamics

To maximize the performance of the aircraft, the aircraft aerodynamic design is optimized by maximizing the propulsive efficiency of the fuel cell aircraft at cruise while applying design constraints on bank angle, climb rate and stall speed. These requirements push the aircraft design towards a design with high wing area and high aspect ratio. Table 2 lists some of the aerodynamic design characteristics of the demonstrator aircraft.

Table 2
Specifications of the demonstrator aircraft

Aircraft specification	Value
Wing area (dm^2)	188
Aspect ratio	23
Wing span (m)	6.58
Tail area (dm^2)	45.5
Length (nose to tail) (m)	2.38
Mass (kg)	16.4
Propeller diameter (cm)	55.9
Propeller pitch (cm)	50.8
Static thrust/weight	0.165
Cruise airspeed ($m\,s^{-1}$)	14.5

The wing is made up of a SD-7032 airfoil with varying taper and twist. The SD-7032 was chosen as compromise between high lift to drag ratio, high thickness ratio and excellent stall characteristics. Because the weight of the aircraft is dominated by the weight of the fuel cell system, the structural weight penalty that goes along with high wing area and aspect ratio is overcome by the improved lifting surface efficiency. The constraint on wing planform aspect ratio is set by a minimum Reynolds number constraint of $Re = 275{,}000$ for the SD-7032 airfoil. To improve the span efficiency, taper and linear washout is added to the outer section of each wing.

A two view drawing of the demonstrator aircraft is shown in Fig. 9. The demonstrator aircraft utilizes a pusher propeller design since a more aggressive rear fuselage taper can be facilitated with a pusher design. Aerodynamic simulation of the entire aircraft shows that the increased rear taper improves the aircraft lift to drag ratio by roughly 8%.

3.2. Aircraft structures

The demonstrator aircraft is constructed from a tubular 6061-T6 aluminum space frame with a roll-wrapped carbon fiber tubular spar. The tail booms are constructed of roll-wrapped carbon fiber tubing, bonded to the spar with aluminum lugs. The fuselage is a non-structural fairing of fiberglass and Nomex honeycomb (Hexcel, Stamford, CT) construction. The wing and tail surfaces are balsa-sheeted polystyrene foam, covered with adhesive film (Monocote, Hobbico Inc., Champaign, IL) The main landing gear are machined out of 6061-T4 aluminum and the

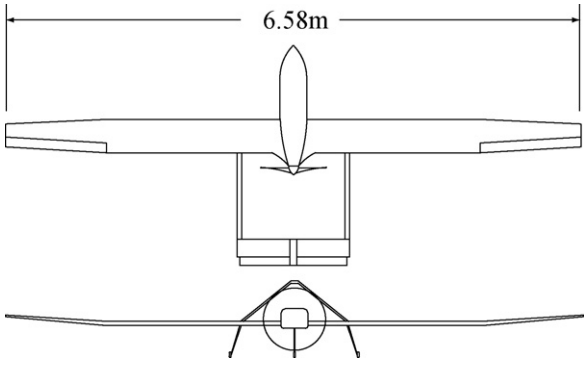

Fig. 9. Two view drawing of fuel cell powered aircraft.

front gear is constructed of tubular fiberglass with a machined 6061-T6 fork.

3.3. Stability and controls

Because the fuel cell aircraft has a much lower power to weight ratio compared to conventionally powered small aircraft, the fuel cell demonstrator is designed for low-speed, stable, level flight with slow maneuvering. This corresponds to a stability number of 1 on the Cooper-Harper scale. The roll stability of the aircraft is set by incorporating polyhedral into the outboard section of the wing. Pitch and yaw stability is set by the size and angle of the "inverted vee" tail. Flaps are included to slow the aircraft for descent and landing.

3.4. Propulsion system

The propulsion system of the aircraft includes the electric motor, motor controller and propeller. The fuel cell provides power to the propulsion system at the fuel cell bus voltage. The aircraft is propelled by a single electric motor and propeller in a pusher configuration. Many of the components of the propulsion system are commercial off the shelf components, but they are specified and combined to maximize the efficiency of the aircraft at cruise.

Generally, the efficiency of the propulsion system increases with increasing propeller diameter and increasing advance ratio [24]. This pushes the propulsion system design towards large diameter propellers with high pitch that are turned by a slow-spinning, high torque motor. Propulsion system designs along this axis are only constrained by the current capacity of the fuel cell powerplant.

The propulsion electric motor (Hacker GmbH, C-50 13XL, Niederhummel, Germany) is a brushless, air cooled motor and incorporates a 6.7:1 planetary reduction between the motor and the propeller. The propeller specified is a 22 in. (56 cm) diameter solid carbon fiber two-bladed propeller with a pitch of 20 in. (51 cm) (Bolly LLC, 22 × 20, Elizabeth West, South Australia).

4. Aircraft and powerplant performance

Because of the low specific power of small scale fuel cell powerplants, the performance of the fuel cell demonstrator aircraft is power limited. The performance of the aircraft is therefore highly dependent on the weight and drag of the aircraft and on the performance of the fuel cell powerplant. In this section, the performance of the aircraft and powerplant systems are analyzed using test data gathered from the demonstration aircraft.

4.1. Aircraft weight breakdown

Fig. 10 shows the measured weight breakdown of the fuel cell demonstrator aircraft. The fuel storage and propulsion systems of the aircraft accounts for roughly 57% of the total aircraft weight. For all fuel cell aircraft designed or constructed to date, including this aircraft, the weight of the aircraft is dominated by the weight of the fuel cell and balance of plant [13,15–17]. For

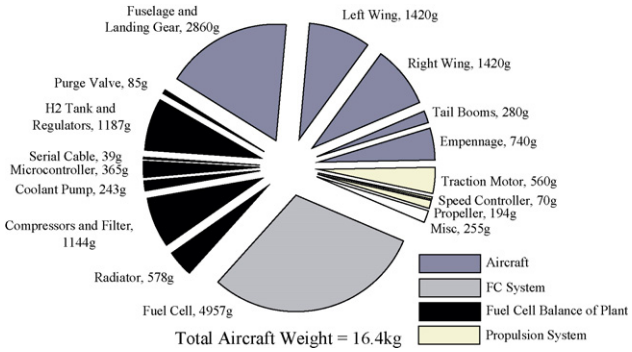

Fig. 10. Weight breakdown for the fuel cell demonstrator aircraft.

smaller fuel cell aircraft this effect occurs because many fuel cell components are heavy at such a small scale. For instance, the hydrogen tank used for the demonstrator aircraft is 1.4% hydrogen by weight. At larger scales, it is possible to manufacture tanks that are >12% hydrogen by weight [25]. Commercially available fuel cell systems at the 500 W scale are not generally intended for mobile applications, and are therefore not weight optimized.

4.2. Flight testing

Flight testing is an integral part of the project because it allows observation of the fuel cell powerplant under real-world operating conditions, it provides a functional test for all of the aircraft systems, and it allows for final validation of the models and assumptions used during design. Fig. 11 shows some of the data collected during a short, high-performance circuit flight test. The flight test is divided into taxiing (0–27 s), climb (27–72 s), descent (72–110 s) and landing (110–160 s) sections. During the beginning of the taxi section, the airspeed and altitude are within measurement error of zero and the fuel cell is at its idling condition. At 10 s, the pilot begins to take off and the fuel cell goes to its maximum power condition. The aircraft accelerates and takes off. As the aircraft climbs, the airspeed and altitude increase as the fuel cell powerplant provides peak power. At the time of 88 s, the pilot lowers the motor command and the aircraft begins to

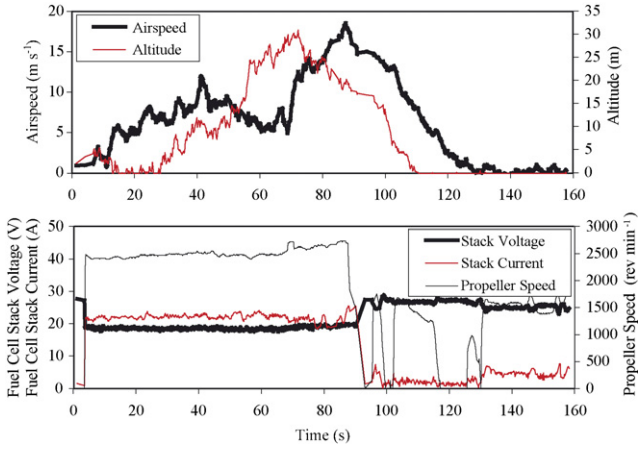

Fig. 11. Representative flight test results for fuel cell powered circuit flight.

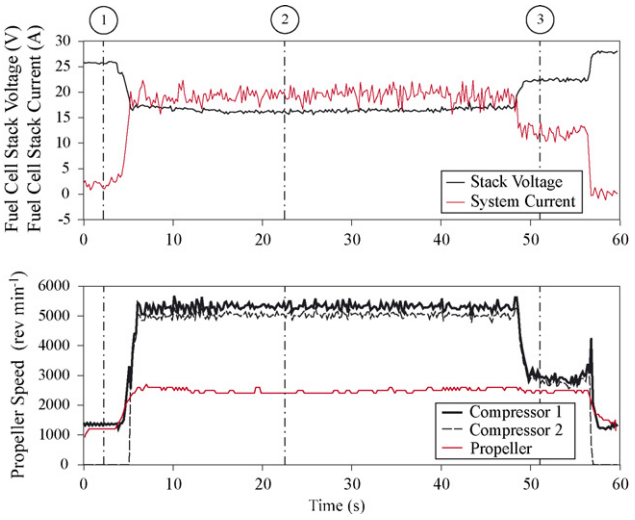

Fig. 12. Representative flight test results for fuel cell powered straight-line flight 4.

descend. At approximately 110 s, the aircraft touches down and coasts to a stop.

Fig. 12 shows the behavior of the aircraft powerplant during a typical straight-line test flight. This data set is from a short, straight-line flight test of 80 s duration and 1200 m distance. The purpose of this test flight was aircraft trim and cruise testing. At the beginning of the flight, the aircraft is stationary on the airfield and the fuel cell is in a low power idle condition. At a time of 3.7 s, the pilot begins to ramp up the current command and the propeller speed increases from the idle condition. The full-power propulsion system current and voltage is reached at 5.2 s. The air supply compressors are then controlled to supply their maximum airflow during the takeoff and climb portions of the flight test. At a time of 48 s, the aircraft stops its high power climb and begins to cruise. The aircraft cruises for 8–10 s and begins to descend and land after the 57 s mark.

4.3. Component power consumptions

A number of points are labeled on Fig. 12. These conditions represent the primary modes of use of the fuel cell powerplant in the UAV application. Point 1 corresponds to the idle condition. Point 2 is a high power condition that occurs during climbing and acceleration. Point 3 is the nominal cruise condition. In each case the performance and efficiency of the powerplant subsystems have been measured and analyzed in greater detail using the results of in-flight, bench-top and wind tunnel testing [26]. These results are presented as Sankey diagrams in Figs. 13–15. Uncertainty analysis is performed using the methods of Kline and McClintock and uncertainties are represented using standard deviations.

At the idle condition the fuel cell is only producing the power required to idle the balance of plant and aircraft controls, as shown in Fig. 13. Almost no net electricity is produced by the fuel cell powerplant as the standby power of the propulsion system is less than 1 W. The input to the fuel cell powerplant is 1.26 Standard L min^{-1} of hydrogen gas. This flow has a lower

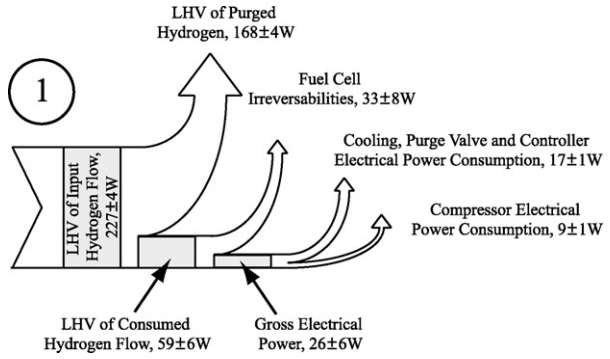

Fig. 13. Propulsion system losses at the idle condition.

heating value (LHV) of 227 W. As shown in Fig. 13, the primary source of losses for the aircraft at idle is the anode purge. The time averaged LHV of the anode purge flow is 168 W. Very little electrical power is generated by the fuel cell because very little electrical power is required to run the balance of plant at idle. As shown in Fig. 12, only compressor 1 is rotating to provide air to the fuel cell stack. This reduces the amount of power consumed by the fuel cell balance of plant to only 26 W.

During the acceleration and climb phase, Point 2 of Fig. 14, the fuel cell powerplant is producing near its maximum power. The LHV of the input hydrogen flow is 1197 W, and the hydrogen utilization of the fuel cell is >88%. The net output power of the fuel cell powerplant is 323 W out of a maximum fuel cell output power of 465 W. The efficiency of the electric motor and motor

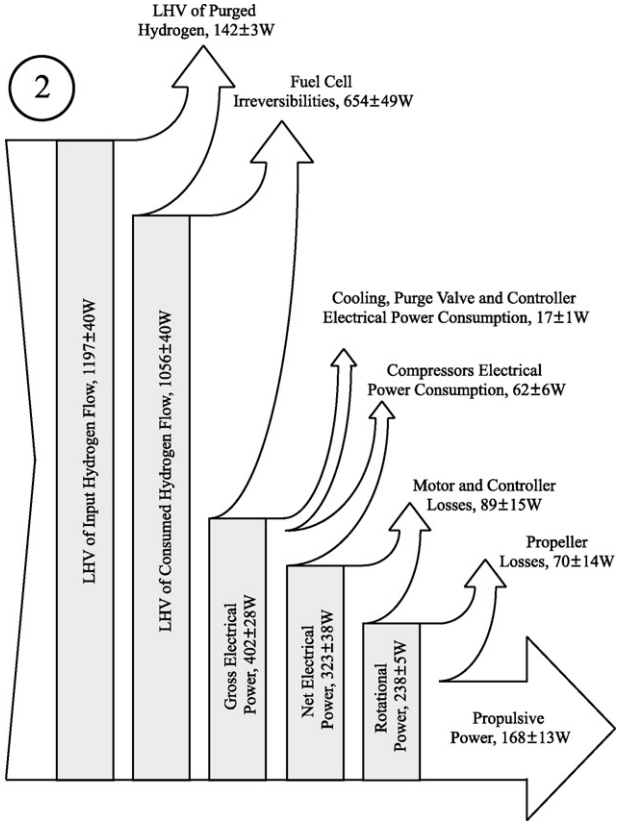

Fig. 14. Propulsion system losses at the high power condition.

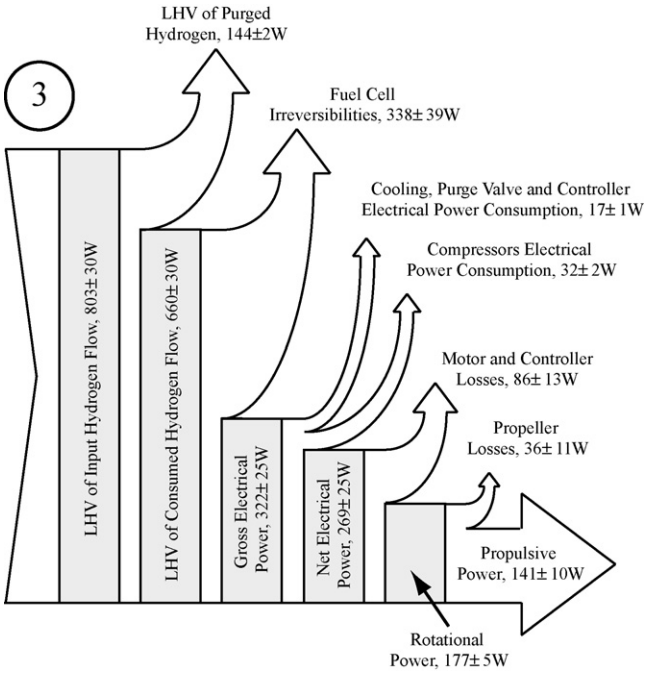

Fig. 15. Propulsion system losses at the cruise condition.

controller is 74% and the efficiency of the propeller is 70%. The efficiency of the propeller is relatively low because of the low speed of the aircraft and low advance ratio at this flight condition. This leads to a relatively low propulsion system efficiency of 14%.

Finally, at the cruise condition, the aircraft is holding steady altitude of approximately 10 m and a steady airspeed of 13.6 m s^{-1}. This cruise condition is faster and at a lower angle of attack than the calculated highest efficiency flight condition, but it is a condition of steady level flight achieved during flight testing. At this condition, shown in Fig. 15, the propulsive power of the aircraft is 84% of the propulsive power at Point 2. At cruise, the electric motor and motor controller is 66% efficient and the propeller is 80% efficient. When compared to the higher power condition, the efficiency of the electric motor is lower because it is functioning at a lower duty cycle, and the propeller efficiency is higher because it is functioning at a higher advance ratio. The total propulsion system efficiency from input hydrogen flow to propulsive power is 18%.

5. Discussion

The results of the flight and laboratory testing show that the fuel cell aircraft has demonstrated the feasibility of fuel cell propulsion of small UAVs. The aircraft is capable of high power acceleration and climb as well as steady cruise flight. Based on the measured capacity of the on-board hydrogen tank (192 Standard L), the aircraft is capable of 43 min of cruising flight. At a constant tank size, the endurance of the aircraft is limited by the efficiency of the propulsion system. The climb and acceleration rate of the aircraft is limited by the propulsive power output of the propulsion system. By reducing the losses or improving the efficiency of the propulsion system, the performance of the aircraft can be improved for all of these metrics.

In all of the flight conditions analyzed in the previous section, there are consistent sources of large losses. By increasing the hydrogen utilization to 99%, as has been possible in other applications [27], the endurance of the aircraft at cruise can be improved to roughly 52 min. The fuel cell powerplant is another large source of losses. The fuel cell powerplant converts 34% of the total hydrogen LHV to output electrical energy at cruise and 33% at high power. This efficiency is comparable to the 35–36% efficiency that has been reported for other small PEM fuel cells [27–29]. The balance of plant power consumption represents 15% of the gross electrical output power of the fuel cell at cruise. This compares favorably to the 20–35% that has been reported in the literature [28–30]. The efficiency of the electric motor is much lower than was predicted by the models supplied by the motor manufacturer. An improved electric motor with efficiencies closer to 80% at cruise would improve the endurance and climb rate of the aircraft. Still the fuel to rotational energy efficiency of the fuel cell powerplant at cruise is 18% (in terms of hydrogen HHV). Again, this compares favorably to an efficiency of 13% for a 500 W, 2-stroke combustion engine (in terms of the HHV of octane) [31]. The fixed pitch propeller requires a compromise between the propeller efficiency during low speed climb and during cruise. For this aircraft the propeller was chosen to maximize efficiency at cruise. A variable pitch propeller would allow for higher efficiency at both the cruise and high power flight conditions.

6. Conclusions

Fuel cell aircraft are an important application for fuel cells because fuel cells are an enabling technology for very long-endurance aircraft. To date, nearly all of the investigations into the design, construction, and performance of fuel cell aircraft have been primarily high-level and conceptual. The construction and experimental evaluation of a fuel cell aircraft has enabled the validation of design models using real-world performance data in addition to the evaluation and the demonstration of a new class of fuel cell vehicle. The results of this study have already been extended to studies of larger, more utilitarian, and much longer endurance aircraft [4].

The fuel cell demonstrator aircraft incorporates a 500 W PEM fuel cell powerplant with an advanced balance of plant including variable cathode flow rate control, liquid cooling, self-humidification and variable period anode purging. The aircraft structure and aerodynamics have been designed incorporating the opportunities and constraints of the fuel cell powerplant. Optimization of the aircraft and propulsion system has produced a stable and efficient experimental platform for evaluation of the fuel cell aircraft concept.

Low level analysis of the performance and efficiencies of the powerplant and propulsion components have allowed for identification of the sources of losses within the aircraft systems. A comparison of the propulsion system performance to the state of the art highlights mechanisms for improving the aircraft performance by improving subsystem performance.

The results of this study are very promising as a proof of the fuel cell aircraft concept. The fuel cell demonstrator aircraft has performed well in test flights and shows the promise of fuel cell aircraft to accomplish new missions with improved effectiveness and environmental performance.

Acknowledgements

This work was funded in part by the National Aeronautics and Space Administration University Research Engineering and Technology Institute at the Georgia Institute of Technology.

The authors would like to thank the research engineers at the Georgia Tech Research Institute Aerospace, Transportation and Advanced Systems Laboratory and the Aerospace Systems Design Laboratory for their expertise and assistance.

The authors would also like to thank Joshua Nelson and L. Scott Miller of the Wichita State University Department of Aerospace Engineering for performing propeller testing and data reduction.

References

[1] S. Tomazic, A. Vugrinec, P. Skraba, Proceedings of the 10th Mediterranean Electrotechnical Conference, Limassol, Cyprus, May 29–31, 2000.
[2] B. Keidel, Auslegung und Simulation von hochfliegenden, dauerhaft stationierbaren Solardrohnen, Technischen Universität München, 2000.
[3] C. Cadou, N. Moulton, S. Menon, Proceedings of the 41st AIAA Aerospace Sciences Meeting and Exhibit, Reno, Nevada, January 6–9, 2003, 2003-671.
[4] B.A. Moffitt, T.H. Bradley, D.E. Parekh, D.N. Mavris, Proceedings of the Sixth AIAA Aviation Technology, Integration and Operations Conference 2006-7701, Wichita, Kansas, September 25–27, 2006.
[5] R.M. Sullivan, J.L Palco, R.T. Tornabene, B.A. Bednarcyk, L.M. Powers, S.K. Mital, L.M. Smith, X.-Y.J Wang, J.E. Hunter, Engineering analysis studies for preliminary design of lightweight cryogenic hydrogen tanks in UAV applications, NASA/TP-2006-214094, 2006.
[6] M. Anderman, Brief assessment of improvements in EV battery technology since the BTAP June 2000 report. California Air Resources Board, 2003.
[7] E.D. Sexton, J.B. Olson, Proceedings of the 13th Annual Battery Conference on Applications and Advances, Long Beach, California, January 11–13, 1998.
[8] F. Mitlitsky, B. Myers, A.H. Weisberg, Proceedings of the 1996 Fuel Cell Seminar, Kissimmee, Florida, November 17–20, 1996.
[9] K.A. Burke, High energy density regenerative fuel cell systems for terrestrial applications, NASA/TM-1999-209429, 1999.
[10] K.A. Burke, Unitized regenerative fuel cell development, NASA/TM-2003-212739, 2003.
[11] M. Asselin, An Introduction to Aircraft Performance, AIAA, Reston, Virginia, 1997.
[12] J. Youngblood, T. Talay, Proceedings of the Second AIAA International Very Large Vehicles Conference, Washington DC, May 17–18, 1982, 1982-0811.
[13] A. Himansu, J.E. Freeh, C.J. Steffen, R.T. Tornabene, X.-Y.J. Wang, Hybrid solid oxide fuel cell/gas turbine system design for high altitude long-endurance aerospace missions, NASA/TM-2006-214328, 2006.
[14] W.H. Wentz, A.S. Mohamed, SAE Trans. J. Aerospace (2004) 1–16, 2004-01-1803.
[15] L.L. Kohutt, P.C Schmitz, Fuel cell propulsion systems for an all-electric personal air vehicle, NASA TM-2003-212354, 2003.
[16] B. Scheppat, Betriebsanleitung für das brennstoff-zellenbetriebene Modellflugzeug, Fachhochschule Wiesbaden, 2004.
[17] J. Kellogg, Fuel cells for micro air vehicles, Joint Service Power Exposition, Tampa, Florida, May 2–5, 2005.
[18] California State University Press Release, Cal State L.A.'s fuel-cell plane passes key flight test, September 1, 2006.
[19] AeroVironment Press Release, AeroVironment flies world's first liquid hydrogen-powered UAV, June 28, 2005.
[20] B.A. Moffitt, T.H. Bradley, D. Parekh, D. Mavris, Proceedings of the 44th AIAA Aerospace Sciences Meeting and Exhibit, Reno, Nevada, January 9–12, 2006, 2006-0823.
[21] T.H. Bradley, B.A. Moffitt, D. Parekh, D. Mavris, Proceedings of the Fourth International ASME Conference on Fuel Cell Science, Engineering and Technology, Irvine, California, June 18–21 2006.
[22] H.P. Dhar, Near ambient unhumidified solid polymer fuel cell, US Patent No. 5,242,764, September 7, 1993.
[23] T.A. Zawodzinki, C. Derouin, S. Radzinski, R.J. Sherman, V.T. Smith, T.E. Springer, S. Gottesfeld, J. Electrochem. Soc. 140 (1993) 1041–1047.
[24] J.T. Lowry, Performance of Light Aircraft, AIAA, Reston, Virginia, 1999.
[25] F. Mitlitsky, A.H. Weisburg, B. Myers, U.S. DOE Hydrogen Program 1999 Annual Review Meeting, Lakewood, Colorado, May 4–6, 1999.
[26] M. Merchant, L.S. Miller, Proceedings of the 44th AIAA Aerospace Sciences Meeting and Exhibit, Reno, Nevada, January 9–12, 2006, 2006-1127.
[27] J.J. Hwang, D.Y. Wang, N.C. Shih, J. Power Sources 141 (2005) 108–115.
[28] J.J. Hwang, D.Y. Wang, N.C. Shih, D.Y. Lai, C.K. Chen, J. Power Sources 133 (2004) 223–228.
[29] T. Susai, A. Kawakami, A. Hamada, Y. Miyake, Y. Azegami, J. Power Sources 92 (2001) 131–138.
[30] P. Atwood, S. Gurski, D.J. Nelson, K.B. Wipke, Proceedings of the Society of Automotive Engineers 2001 World Congress, Detroit, Michigan, March 5–8, 2001, 2001-01-0236.
[31] C. Cadou, T. Sookdeo, N. Moulton, T. Leach, Proceedings of the AIAA First Technical Conference and Workshop on Unmanned Aerospace Vehicles, Portsmouth, Virginia, May 20–23, 2002, 2002-3448.